Improved Global Rational Approximation Macromodeling Algorithm for Networks Characterized by Frequency-Sampled Data

Mark Elzinga, Kathleen L. Virga, *Senior Member, IEEE*, and John L. Prince, *Fellow, IEEE*

***Abstract*—Recently, the demand for high-performance wireless designs has been increasing while simultaneously the speed of high-end digital designs have crossed over the gigahertz range. New simulation tools which accurately characterize high-frequency interconnects are needed. This paper presents improvements to a new macromodeling algorithm described in [1]. The algorithm employs curve-fitting techniques to achieve a pole-residue approximation of the frequency-sampled network. The frequency sampled S-parameters or Y-parameters can be obtained from measurement or full-wave simulation to characterize the frequency-dependent interconnects behavior. The improvements extend the approach to lossless structures, increase its accuracy with pole-clustering, and ensure its validity with a passivity test. This paper addresses some of the special considerations that must be made to the method so it can efficiently and accurately be applied to lossless circuits and structures. The resulting algorithm is now capable of accurately extracting a wide-band frequency domain macromodel from frequency-sampled data for either LC circuit (lossless) or RLC circuits (lossy). The frequency-domain macromodel can be linked to a SPICE circuit simulator for mixed signal circuit analysis using RF, analog, and digital circuits. The circuit can be simulated in the time domain using recursive convolution.**

***Index Terms*—Curve-fitting, interconnect simulation, macromodeling, measured data, passivity, poles, pole-residue approximation, rational approximation, S-parameters, transfer functions, transient simulation, transmission lines, Y-parameters.**

I. Background and Introduction

THE DIFFICULTIES with performing accurate broadband interconnect simulation is that typical full-wave techniques are often too slow and are incompatible with existing circuit simulators. The concept of macromodeling has been used in order to strike an optimal balance between accuracy, flexibility, and speed. Macromodeling is the process that allows a complicated structure that is difficult or time-consuming to simulate to be represented accurately by an approximate system that can easily be simulated. An interconnect macromodel defines the behavior of an n-port (where n is the number of input plus output terminals) interconnect system. For passive structures, it is desired that the resulting macromodel be linear and passive. Frequency-domain macromodels in the form of global rational function approximations to the frequency-domain data can potentially represent an interconnect system in the frequency domain and give accurate time-domain results when combined with other circuit elements in a modified SPICE simulator. This facilitates the simulation of mixed signal systems that contain microwave, RF, analog, and digital circuits all within the same high-density circuit package.

To quantify the behavior of the n-port, a macromodeling process utilizes information about the relations between the input and output responses of a circuit or structure. Some types of macromodeling, including asymptotic waveform expansion (AWE) [2], Padé via Lanczos (PVL) [3], and Passive Reduced-order Interconnect Macromodeling Algorithm (PRIMA) [4] can use circuit models obtained through Partial-Element Equivalent Circuit (PEEC) [5] or other methods. PEEC discretizes a structure into RLC networks to approximate a full-wave distributed circuit model. The objective of AWE, PVL, and PRIMA in reducing simulation time is based upon reducing the order (i.e., number of elements) of the circuit. These macromodeling techniques use the original circuit characterized by the modified nodal admittance (MNA) matrix [6] as the input "information" to obtain a reduced-order macromodel. One limitation to these techniques is that they are not readily applied to networks that have been characterized with measured or tabulated data.

Some macromodeling approaches use frequency-sampled data to characterize the n-port system. The advantage of this approach is that the characterizing "information" may come from a diversity of sources including full-wave simulation and network analyzer measurements. A straightforward approach to obtain transient simulation of frequency sampled networks is to use the inverse fast Fourier transform (FFT) and obtain the time-domain impulse response. For each time step the time-domain impulse response is convolved with the input waveform to obtain the system response. The drawback to this approach is the computational cost of the convolution process. One class of frequency-sampled macromodeling [7], [8] expands existing macromodeling techniques like complex frequency hopping (CFH) to handle networks characterized by sampled data. CFH is based on Padé approximations at multiple frequency points. The method used in [7] overcomes the problem of the inverse FFT and convolution method by effectively interpolating the frequency response of the system using CFH. The drawback to this approach is the need to perform an FFT to obtain the frequency-domain corollary to the time-domain input functions and then use an inverse FFT for every time-domain simulation

Manuscript received June 15,2000. This work was supported in part by SRC under Contract 97-MP-086 through CEPR, the University of Arizona, Tucson.

The authors are with the Center for Electronic Packaging Research, Department of Electrical and Computer Engineering, University of Arizona, Tucson, AZ 85721 USA (e-mail: prince@ece.arizona.edu).

Publisher Item Identifier S 0018-9480(00)07412-3.

performed. The technique is effective for ideal linear sources, but cannot be applied to circuits containing nonlinear driving devices such as MOSFETs.

The CFH technique used in [8] allows for simulation with nonlinear devices. The difficulty in this method is that for every moment, a corresponding derivative of each Y parameter must be computed using numeric integration across the entire time spectra. This process has to be done for every frequency point, which can be cumbersome for networks with a large number of sample points, a high order of approximation, or networks with many ports.

Another approach to frequency-sampled macromodeling that is discussed in [1], [9]–[11] involves using direct rational approximations instead of a moment-matching approach. The macromodels obtained from direct rational approximations can be used in conjunction with recursive convolution [12] to efficiently simulate interconnects along with nonlinear devices in a modified version of SPICE [13]. The method in [10] partitions the data set into sections to avoid problems associated with ill-conditioning and obtains low-order rational approximations for each set. At the end of each section the resulting approximation is added to the approximation obtained from the last section and the resulting approximation is subtracted from the original data for the next iteration. One of the drawbacks of this approach is that each section adds more pole-residue terms to the approximation. Consequently, the overall model has an artificially large number of poles. A separate computation is required in order to obtain a reduced-order model.

The method in [11] uses a novel approach that recursively computes pole–zero pairs. The algorithm uses a least squares curve-fitting technique to find an initial first-order pole–zero approximation, then creates a new data set used for the next approximation by dividing the original data by the first-order approximation. The algorithm calculates a new pole–zero pair with each iteration. The problem with the method discussed in [11] is that the matrix systems formulated in this approach are only valid for real poles, which restricts the application of this technique to RL and RC circuits.

In [14], Brittingham shows the viability of a global rational approximation technique that is much simpler than a section-by-section or iterative approach. Brittingham showed that by constraining the poles of the rational approximation to be real or complex conjugate pairs, it "*forestalls failure of the method even when the number of poles is very large.*" The approach discussed in [9] incorporates matrix equations that guarantee this condition. However, the matrix systems formulated introduce unnecessary ill-conditioning to the approximations by using squared terms of ω in the numerator and denominator polynomials. Another limitation of this method is that the residue calculation for complex conjugate pole pairs may lead to less accurate results. The new technique presented in [1] overcomes these limitations.

The present paper expands the work of the macromodeling algorithm discussed in [1] by adding some special considerations that must be made for lossless (LC) structures. This paper also presents additional performance enhancements. The accuracy of the overall algorithm is improved using pole-clustering. A method to test for passivity of the frequency-domain macromodels is described. Section II describes the macromodeling algorithm as it applies to lossless structures. An algorithm for pole-clustering is discussed in Section III. A method to test for passivity is presented in Section IV. In Section V, examples of the accuracy and usage of the algorithm for several different structures are given. Section VI provides some conclusions.

II. Application to Lossless Networks

The macromodeling algorithm consists of two steps. The first step is to use rational functions given as a ratio of polynomials to approximate the frequency-domain behavior of the elements of the Y-matrix, or admittance matrix, of the n-port structure. The second step involves recasting the ratio of polynomials representation for the Y-matrix elements into a new form using the partial expansion representation to obtain the residues. In order obtain a suitable model for lossless networks, several important modifications to the derivation and equations presented in [1] must be made.

The first step in the process is to extract the poles of the system given the frequency-sampled data. Given the ijth admittance matrix element as a function of frequency, $Y_{ij}(s)$, a rational approximation is made as follows:

$$Y_{ij}(s) = \frac{a_0 + a_1 s + a_2 s^2 + a_3 s^3 + \cdots + a_{n-1} s^{n-1} + a_n s^n}{b_0 + b_1 s + b_2 s^2 + b_3 s^3 + \cdots + b_{n-1} s^{n-1} + b_n s^n} \tag{1}$$

where $s \in (j\omega_1, j\omega_2, \cdots, j\omega_{f-1}, j\omega_f)$, f is the total number of frequency points, and n is the order of the denominator and numerator polynomials. The macromodel approach is formulated for the Y-matrix elements, since the modified version of SPICE mentioned earlier uses the partial fraction expansion form of the Y-matrix elements. This ability to generate macromodels of the elements of the Y-matrix for high-frequency structures is important for the simulation of systems for digital, mixed-signal, and RF applications.

Matrix equations of the form $[A][x] = [B]$ are formulated by multiplying both sides of (1) and then separating the real and imaginary parts of the result. For example, if n is even and $Y_{ij} = Y_r + jY_i$, the result is

$$\begin{aligned} &a_0 + a_2 s^2 + \cdots + a_n s^n \\ &\quad = Y_r b_0 + jY_i s b_1 + Y_r b_2 s^2 + \cdots + jY_i b_{n-1} s^{n-1} + Y_r s^n. \end{aligned} \tag{2}$$

The result of this formulation for other cases is given in [1].

For lossless structures it is known that the elements of the Y-matrix are purely imaginary, thus $\mathrm{Re}\{Y_{ij}\} = 0$. Consequently, several columns of the matrix on the left-hand side that is formulated in the first step of the process will be zero. In order to obtain a solution to the system of equations, these columns must be eliminated. Since all of the poles in a lossless network are purely imaginary and come in conjugate pairs, the order of the polynomials, specified by n, in (1) must be even. The resulting form of the system of equations for a lossless network is given by (3) at the top of the following page, where the additional numerical subscript on Y indicates frequency points that range from 1 to f. The system of equations given in (3) can

$$\begin{bmatrix} \omega_1 & \omega_1^3 & \omega_1^5 & \cdots & \omega_1^{n-1} & -Y_{1i} & Y_{1i}\omega_1^2 & -Y_{1i}\omega_1^4 & \cdots & (-1)^{n/2}Y_{1i}\omega_1^{n-2} \\ \omega_2 & \omega_2^3 & \omega_2^5 & \cdots & \omega_2^{n-1} & -Y_{2i} & Y_{2i}\omega_2^2 & -Y_{2i}\omega_2^4 & \cdots & (-1)^{n/2}Y_{2i}\omega_2^{n-2} \\ \vdots & \vdots & \vdots & \cdots & \vdots & \vdots & \vdots & \vdots & \vdots & \vdots \\ \vdots & \vdots & \vdots & \cdots & \vdots & \vdots & \vdots & \vdots & \vdots & \vdots \\ \vdots & \vdots & \vdots & \cdots & \vdots & \vdots & \vdots & \vdots & \vdots & \vdots \\ \omega_f & \omega_f^3 & \omega_f^5 & \cdots & \omega_f^{n-1} & -Y_{fi} & Y_{fi}\omega_f^2 & -Y_{fi}\omega_f^4 & \cdots & (-1)^{n/2}Y_{fi}\omega_f^{n-2} \end{bmatrix} \cdot \begin{bmatrix} a_1 \\ -a_3 \\ a_5 \\ \vdots \\ (-1)^{n/2+1}a_{n-1} \\ b_0 \\ b_2 \\ b_4 \\ \vdots \\ b_{n-2} \end{bmatrix} = \begin{bmatrix} (-1)^{n/2}Y_{1i}\omega_1^n \\ (-1)^{n/2}Y_{2i}\omega_2^n \\ \vdots \\ \vdots \\ \vdots \\ (-1)^{n/2}Y_{fi}\omega_f^n \end{bmatrix} \tag{3}$$

be used to obtain the coefficients a_k and b_k and thus the frequency-domain macromodel representation for the respective Y-matrix element.

The second step of the algorithm is effectively a partial fraction expansion of (1), except that (unstable) right half-plane (RHP) poles are removed after factoring the denominator. If $Y_{ij}(s)$ is the network parameter, and m the number of left half-plane (LHP) poles, then

$$Y_{ij}(s) = k_\infty + \sum_{a=1}^{m} \frac{k_a}{s - p_a} \tag{4}$$

where $m \leq n$, and n was specified in the first step of the procedure.

A new matrix equation is formulated to calculate k_∞ (a constant) and each residue k_a, for each of the poles, p_a, and the $Y_{ij}(s)$ values. The resulting matrix equation for the lossless case is quite different from the equation for circuits with loss. A lossless structure has purely imaginary conjugate pole pairs and purely real residues. Consequently, (4) becomes

$$\mathrm{Im}\{Y_{ij}(s)\} = \sum_{a=1}^{C} \left(\frac{k_a}{s - p_a} + \frac{k_a}{s - p_a^*} \right) \tag{5}$$

for the lossless case, where C is the number of imaginary conjugate pole pairs. The resulting matrix equation for the calculation of the residues is (6) at the bottom of this page.

The poles and residues for a lossless (LC) macromodel can be generated from (3) and (6). The modifications made to the process of calculating the poles and the residues allow the method to correctly extract macromodels for lossless structures.

III. Pole Clustering

One improvement to the technique is achieved by applying pole-clustering after the poles have been computed for each element of the Y-matrix. The elements of the Y-matrix of a linear network have the same poles. However, numerical errors inherent in the macromodel approximation will result in different Y-matrix elements having similar, yet slightly different pole values. Pole-clustering is a method in which the poles of different Y-matrix elements that closely match are averaged together and then considered as one set of poles. The goal of pole-clustering is to come up with a set of poles that is common to all elements of the Y-matrix in the approximation.

The pole-clustering algorithm is very straightforward. First, all the poles of Y_{11} are compiled into an initial list of poles. The poles of the next Y-matrix element are then determined. Each pole for the new Y-matrix element is then matched with a pole from the initial list. A match is obtained if the difference between the location a pole in the initial list and a pole for new Y-matrix element is below a specified tolerance. If this difference is within tolerance, the initial list is updated with a weighted average of the "clustered" poles. If any new poles cannot be matched with any pole from the initial list, then the initial list is updated with the new pole location. This process of updating the pole list and comparing with the poles for each Y–matrix element is continued for all the elements of the Y-matrix. The pole-clustering algorithm is as follows.

$$\begin{bmatrix} \mathrm{Im}\left\{\frac{1}{s_1 - p_1} + \frac{1}{s_1 - p_1^*}\right\} & \mathrm{Im}\left\{\frac{1}{s_1 - p_2} + \frac{1}{s_1 - p_2^*}\right\} & \cdots & \mathrm{Im}\left\{\frac{1}{s_1 - p_C} + \frac{1}{s_1 - p_C^*}\right\} \\ \mathrm{Im}\left\{\frac{1}{s_2 - p_1} + \frac{1}{s_2 - p_1^*}\right\} & \mathrm{Im}\left\{\frac{1}{s_2 - p_2} + \frac{1}{s_2 - p_2^*}\right\} & \cdots & \mathrm{Im}\left\{\frac{1}{s_2 - p_C} + \frac{1}{s_2 - p_C^*}\right\} \\ \vdots & \vdots & \vdots & \vdots \\ \mathrm{Im}\left\{\frac{1}{s_f - p_1} + \frac{1}{s_f - p_1^*}\right\} & \mathrm{Im}\left\{\frac{1}{s_f - p_2} + \frac{1}{s_f - p_2^*}\right\} & \cdots & \mathrm{Im}\left\{\frac{1}{s_f - p_C} + \frac{1}{s_f - p_C^*}\right\} \end{bmatrix} \cdot \begin{bmatrix} \mathrm{Re}\{k_1\} \\ \mathrm{Re}\{k_2\} \\ \vdots \\ \mathrm{Re}\{k_C\} \end{bmatrix} = \begin{bmatrix} \mathrm{Im}\{Y_1\} \\ \mathrm{Im}\{Y_2\} \\ \vdots \\ \mathrm{Im}\{Y_f\} \end{bmatrix} \tag{6}$$

1) Create a data structure, clustered_poles, that will record the values of clustered poles and which Y parameter(s) they belong to.
2) Start with the first Y parameter, Y_{11}, and copy all the pole values into clustered_poles, and record that these pole values belong to Y_{11}.
3) Let $i = 1$ to the total number of Y-parameters:
   A. Let $k = 1$ to total number of clustered_poles.
      i) Find the closest "matching" pole in Y_i to the kth pole in clustered_poles that minimizes $\dfrac{|\text{clustered\_pole}_k - \text{matching\_pole}_j|}{|\text{clustered\_pole}_k|}$.
      ii) IF the "match" is within tolerance, THEN, computed the weighted average (based on how many Y-parameters currently contain the kth clustered pole) of the kth clustered_pole and the matching pole to compute the updated value of the kth clustered pole value. Next, record that the kth clustered pole is a member of the parameter Y_i.
      OR
      iii) IF not match is possible, THEN add a new pole to the list of clustered_poles. Then record that the new clustered pole is a member of the parameter Y_i.
   B. Scan through clustered_poles, and update array that contains pole values that belong to Y_i.

A tolerance value of 0.5% achieves good results in the clustering process and has been used for the examples presented in this work.

IV. Passivity Testing

Another improvement to the technique is to add the capability to test for passivity. By removing RHP poles, the algorithm does ensure a stable system, but the macromodel is not guaranteed to be passive. If the original data is passive and the approximation is good it is expected that the resulting macromodel will be passive. All the macromodels extracted to date using this algorithm and using an appropriate value of n are passive.

A passive network is a network that is unable to create energy and does contain independent or dependent sources. A network is passive if the Hermitian matrix, $[G]$, whose elements G_{ij} are equal to $(Y_{ij}+Y_{ji}^*/2)$, where i may equal j, is positive semidefinite [15]. This means that $[G] = \text{Re}\{[Y]\}$ when the network is symmetric. For a nonsymmetric network $[G] = \text{Re}\{[Y]\}$ for the diagonal elements and $G_{ij} = (Y_{ij} + Y_{ji}^*/2)$ for the off-diagonal elements. One interesting result of the positive semidefinite nature of $[G]$ is that $\text{Re}\{Y\} > 0$ for all diagonal elements [16]. A matrix can be tested for positive semidefiniteness by performing a simple algorithm called the Pivot Test [16]. This is done by successively pivoting on the diagonal entries in $[G]$, first by pivoting on the first diagonal element G_{11}, then proceeding by pivoting on the second diagonal element G_{22}, and so on. $[G]$ will be positive semidefinite if after the successive pivoting process, the resulting matrix $[G]$ has nonnegative diagonal elements. This passivity test has been applied to lossy networks.

A different passivity test must be used for lossless networks, since passive networks have positive real matrices. One condition for a rational function to be considered a positive real function is that the residues of purely imaginary poles must be positive and real [17]. This concept can be extended to all the elements of the Y-matrix of a lossless network by generating a matrix that represents the residues corresponding to each element of the Y-matrix for the kth pole. If the resulting matrix is not symmetric, the off-diagonal elements are modified to make it symmetric by using $G_{ij} = (k_{ij} + k_{ji})/2$. The matrix will be positive-real if the matrix G is positive semidefinite. Thus if G is positive semidefinite, the macromodel is passive. Note therefore that a necessary condition for passivity is that for all diagonal elements of $[Y]$ of a lossless structure the residues must be positive and real.

V. Examples

In this section, the macromodeling method is applied to several examples. The first example is used to show how the choice of the order of the rational function is important to obtain accurate results. The following two examples show the results of the macromodeling method applied to a simple lossless microstrip structure as well as a more complicated waveguide structure.

Fig. 1 shows how the choice of the order of the polynomials n in the rational function (1) impacts the accuracy of the frequency-domain macromodel for a three-section RLC circuit. This figure compares the real and imaginary values of Y_{11} obtained from SPICE with the values of Y_{11} generated from macromodels with varying orders of n. Fig. 2 compares the average error between the macromodel and the exact value of Y_{11} for the RLC circuit for different values of n. The error is computed by using

$$\text{Error}_{ij}(s_k) = \frac{|Y_{ij}(s_k) - \tilde{Y}_{ij}(s_k)|}{|\overline{Y}_{ij}|} \tag{7}$$

where $\overline{Y}_{ij}$ is the average value of Y_{ij} for all the frequency points s_k, $Y_{ij}(s_k)$ is computed by SPICE at the frequency s_k, and $\tilde{Y}_{ij}(s_k)$ is the value of Y_{ij} at frequency s_k computed by the macromodel. The average error is computed by averaging (7) for all values of i, j, and k. The average error weights the errors in all the Y-matrix elements on an equal basis and does not focus on the error of one element over another.

In the RLC circuit example, for a value of n that is equal to and above the threshold order of five (which happens to be the actual order of Y_{11}), the macromodel results overlay the SPICE results very well. For macromodels that are generated with a value of n that is below the threshold order, the accuracy of the approximation is usually very poor. The macromodels obtained from below-threshold values of n may not even result in a passive macromodel. Macromodels generated using values of much greater than the threshold order are accurate but may contain extra poles that have small residues that arise due to numerical reasons. The threshold order in a real system corresponds to the number of dominant poles.

The improved macromodeling procedure has been applied to a lossless microstrip structure shown in Fig. 3. The lossless mi-

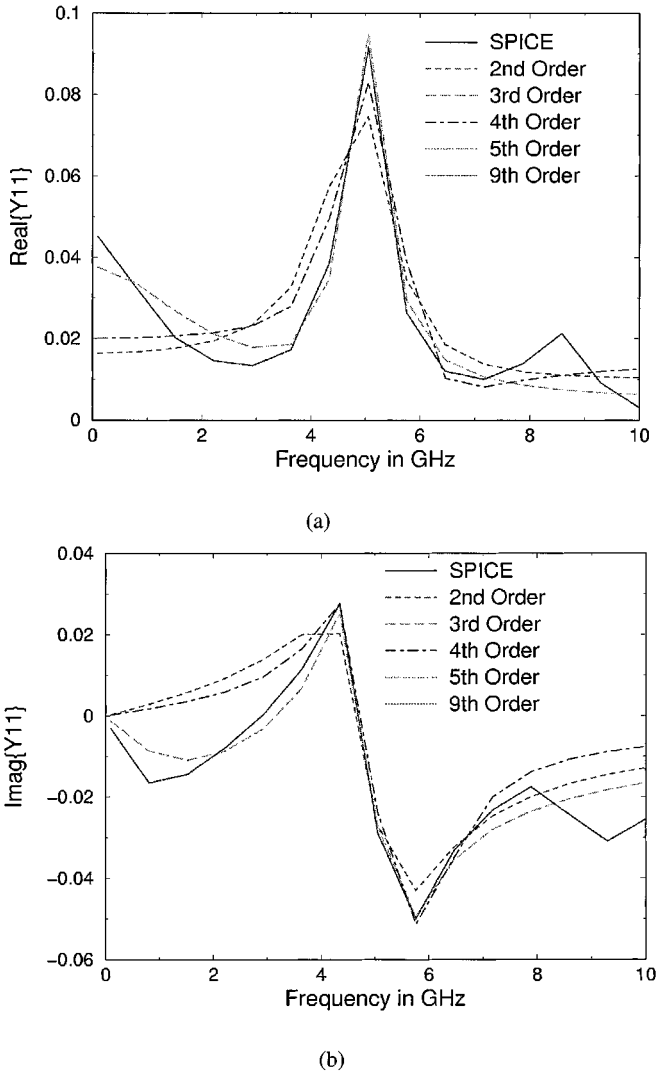

Fig. 1. Frequency domain fit for Y_{11} approximations to an RLC circuit. (a) $\mathrm{Re}\{Y_{11}\}$ and (b) $\mathrm{Im}\{Y_{11}\}$.

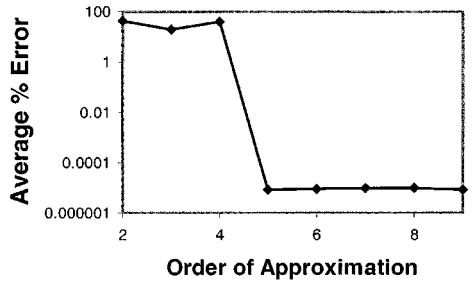

Fig. 2. Average error (log scale) for varying orders of approximation of a three-section RLC circuit.

crostrip is 3 cm long. The microstrip structure was simulated in the frequency domain with a commercial transmission line simulator HP-ADS [18] to extract the Y parameters. This data was used to develop a macromodel of this structure. Fig. 4 compares the elements of the Y-matrix directly computed from HP-ADS with the Y-matrix computed from the macromodel for the case where $n = 12$. These results show that there is excellent agreement between the macromodel and the original HP-ADS data

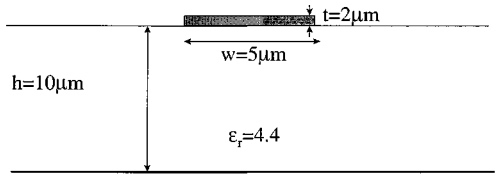

Fig. 3. Dimensions of a lossless microstrip structure.

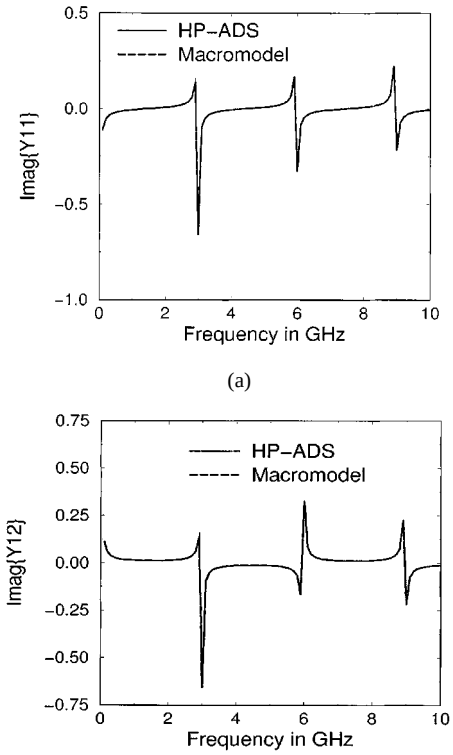

Fig. 4. Comparison of Y-parameters computed by HP-ADS and 12th-order macromodel for lossless microstrip example, (a) $\mathrm{Im}\{Y_{11}\}$ and (b) $\mathrm{Im}\{Y_{12}\}$

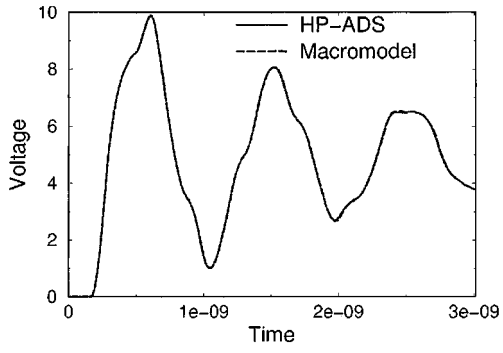

Fig. 5. Transient simulation of the output voltage of a lossless microstrip using HP-ADS and macromodeling technique.

and that a macromodel order of $n = 12$ is sufficient to accurately reconstruct the original data. The macromodel was used in a transient simulation of the microstrip line. The circuit used a 5-V step with a 0.1-ns rise time as a voltage source, a 1-pF capacitor on the output, and a 10-Ω source resistance. Fig. 5

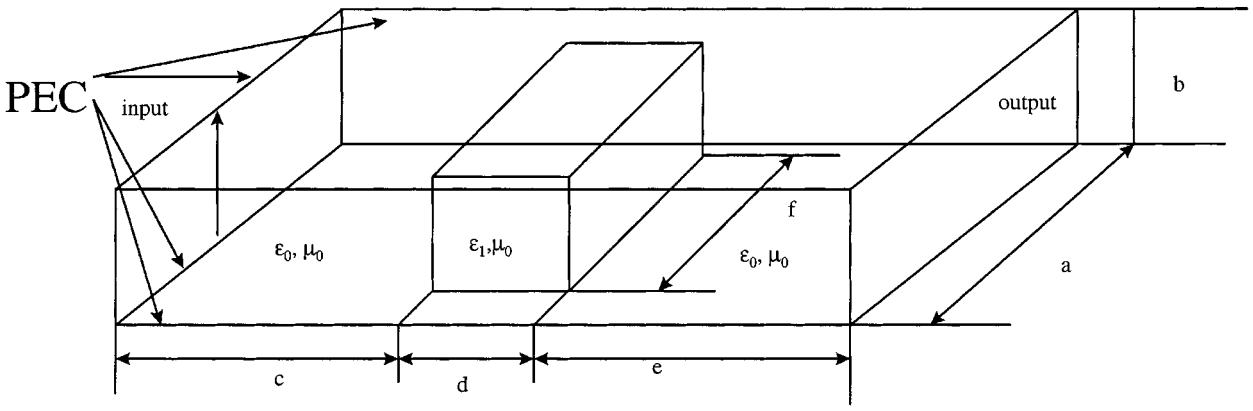

Fig. 6. Parallel-plate waveguide with dielectric post; $a = 14$ mm, $b = 6$ mm, $c = 6.4$ mm, $d = 3.2$ mm, $e = 3.2$ mm, $f = 8$ mm, $\varepsilon_r = 8.2$.

compares the value of the far-end voltage of the line from a direct transient simulation from HP-ADS and a transient simulation using the rational function form of the macromodel in AZSPICE. This figure shows excellent agreement between the original and macromodeled results.

The macromodeling technique was applied to a structure that was modeled using a full-wave simulation approach based upon the solution of Maxwell's equations. This example demonstrates the capability of the technique to obtain an accurate frequency-domain macromodel given full-wave simulation data of a complex structure. A finite-difference frequency-domain (FDFD) full-wave simulator tool [19] was used to obtain the two-port S-parameters of a parallel-plate waveguide structure with a dielectric post, as shown in Fig. 6. The presence of the dielectric post in the waveguide generates higher order modes in the waveguide. The frequency behavior of these modes are neglected when simple equivalent circuit models are used to simulate this structure, and thus it is important to use a full-wave simulation approach to capture the appropriate frequency response.

The FDFD simulation approach can be used to obtain many frequency points, but only a fraction of them are actually needed to obtain a suitable macromodel approximation. To obtain the macromodel, the S-parameters are first converted to Y-parameters using the following transformations [20]:

$$Y_0 = \frac{1}{Z_0} = \frac{w}{\eta_0 d} \tag{8}$$

$$D = \frac{Y_0}{(1+S_{11})(1+S_{22}) - S_{12}S_{21}} \tag{9}$$

$$Y_{11} = D[(1-S_{11})(1+S_{22}) + S_{12}S_{21}] \tag{10}$$

$$Y_{12} = D[-2S_{12}] \tag{11}$$

$$Y_{21} = D[-2S_{21}] \tag{12}$$

$$Y_{22} = D[(1-S_{22})(1+S_{11}) + S_{12}S_{21}] \tag{13}$$

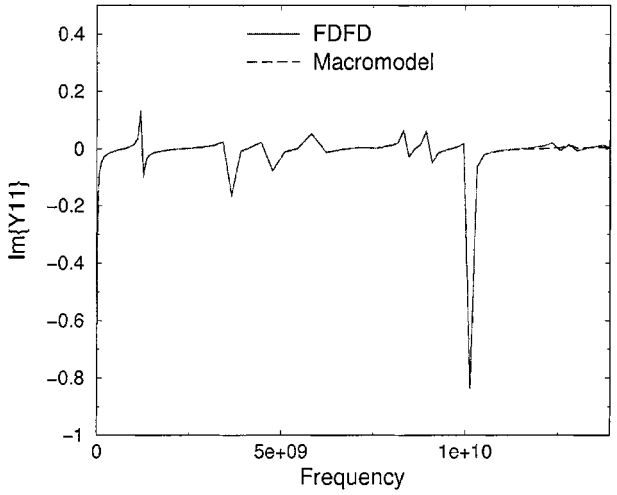

(a)

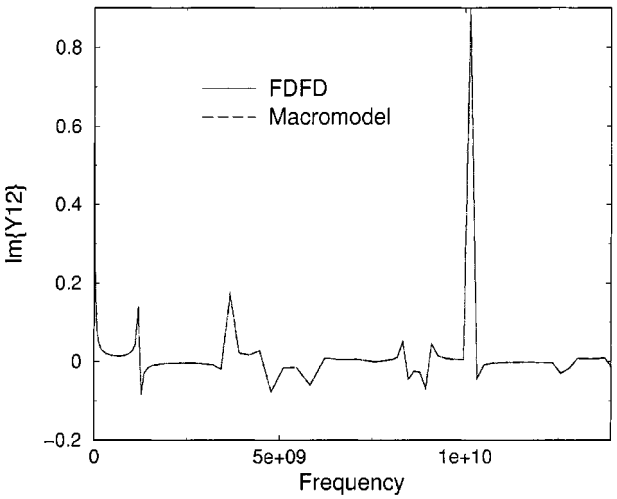

(b)

Fig. 7. Y-parameters computed by FDFD and macromodel ($n = 32$) order for parallel-plate waveguide example. (a) $\mathrm{Im}\{Y_{11}\}$ and (b) $\mathrm{Im}\{Y_{12}\}$

where Z_0 is the waveguide impedance that is used as the reference impedance from which to characterize the S-parameters

of the post. The parameter w is the width, and d is the height of the gap of the parallel-plate waveguide.

The Y-parameters were computed using S-parameter data from the FDFD simulation at 126 frequency points ranging from 100 MHz to 13.9 GHz. A macromodel of the Y-parameters was generated for a value of $n = 32$. Fig. 7 compares the elements of the Y-matrix directly computed from the FDFD simulation and with the values computed from the macromodel. This figure shows that the FDFD results and results obtained from the macromodel are in good agreement. The large fluctuations and resonances in the frequency response are accurately reproduced with the macromodel.

In order to determine the correct order of this model, several different macromodels with were conducted. Polynomial orders of $n = 16, 28, 30$, and 32 were tried. The average error computed from (7) was computed for these cases and compare. When $n = 16$, the average error between the original Y–parameters and the approximate Y–parameters was 91%. When $n = 28$, the error dropped to 83%, and when $n = 30$ order approximation the error dropped to 42%. When $n = 32$, the error dramatically dropped to 0.693%! This example shows that it is important to compute the proper order of n to obtain accurate results and that even a slight increase in n can result in significant accuracy in the resulting macromodel.

VI. Conclusion

With the passivity test, pole-clustering, and the lossless extension, the global rational approximation macromodeling technique has been greatly improved. The new algorithm provides the microwave circuit designer with an improved design tool that can generate accurate frequency-domain macromodels of complex interconnects. For digital, mixed-signal, or RF applications the macromodels enable circuit designers to obtain transient simulations of complex interconnect structures characterized by frequency-sampled data along with nonlinear devices like MOSFETs. By modifying the algorithms associated with the pole-residue calculations, the overall result is a fast and accurate algorithm capable of correctly handling both the lossless and lossy case. The improvements have also increased the accuracy of the pole calculations and provided a method to evaluate passivity of the result.

References

[1] M. Elzinga, K. Virga, L. Zhao, and J. L. Prince, "Pole-residue formulation for transient simulation of high-frequency interconnects using householder LS curve-fitting techniques," *IEEE Trans. Adv. Packag.*, vol. 25, pp. 142–147, May 2000.

[2] L. T. Pillage and R. A. Rohrer, "Asymptotic waveform evaluation for timing analysis," *IEEE Trans. Computer-Aided Des.*, vol. 14, pp. 639–649, May 1990.

[3] P. Feldmann and R. W. Freund, "Efficient linear circuit analysis by Padé approximation via the Lanczos process," *IEEE Trans. Computer-Aided Des.*, vol. 14, pp. 639–649, 1995.

[4] A. Odabasioglu, M. Celik, and L. T. Pileggi, "PRIMA: Passive reduced-order interconnect macromodeling algorithm," *IEEE Trans. Computer-Aided Des.*, vol. 17, pp. 645–653, Aug. 1998.

[5] A. E. Ruehli and H. Heeb, "Circuit models for three-dimensional geometries including dielectrics," *IEEE Trans. Microwave Theory Tech.*, vol. 40, pp. 1507–1516, July 1992.

[6] C. Ho, A. Ruehli, and P. Brennan, "The modified nodal approach to network analysis," *IEEE Trans. Circuits Syst.*, vol. CAS-22, pp. 504–509, June 1975.

[7] R. Sanaie, E. Chiprout, and M. S. Nakhla, "A fast method for frequency and time domain simulation of VLSI interconnects," *IEEE Trans. Microwave Theory Tech.*, vol. 42, pp. 2562–2571, Dec. 1994.

[8] R. Achar and M. S. Nakhla, "Efficient transient simulation of embedded subnetworks characterized by s-parameters in the presence of nonlinear elements," *IEEE Trans. Microwave Theory Tech.*, vol. 46, pp. 2356–2363, Dec. 1998.

[9] W. T. Beyene and J. E. Schutt-Aine, "Efficient transient simulation of high-speed interconnects characterized by sampled data," *IEEE Trans. Comp., Packag. Manufact. Technol. B*, vol. 21, pp. 105–114, Feb. 1998.

[10] L. M. Silveira, I. M. Elfadel, J. K. White, M. Chilukuri, and K. S. Kundert, "Efficient frequency-domain modeling and circuit simulation of transmission lines," *IEEE Trans. Comp., Packag. Manufact. Technol. B*, vol. 17, pp. 505–513, Nov. 1994.

[11] E. C. Chang, "Transient simulation of lossy coupled transmission lines using iterative linear least squares fitting and piecewise recursive convolution," *IEEE Trans. Circuits Syst. I*, vol. 43, Nov. 1996.

[12] S. Lin and E. Kuh, "Transient simulation of lossy interconnects based on the recursive convolution formulation," *IEEE Trans. Circuits Syst.*, vol. 39, pp. 879–892, Nov. 1992.

[13] M. Celik, "AZSPICE, Modified from Berkely SPICE 3F4," Ctr. Electron. Packag. Res., Univ. Ariz., Tucson, 1996.

[14] J. N. Brittingham, E. K. Miller, and J. L. Willows, "Pole extraction from real-frequency information," *Proc. IEEE*, vol. 68, pp. 263–273, Feb. 1980.

[15] W. H. Kim and H. E. Meadows, *Modern Network Analysis*. New York: Wiley, 1971, p. 195.

[16] H. W. Brinkmann and E. A. Klotz, *Linear Algebra and Analytic Geometry*. Reading, MA: Addison-Wesley, 1971, pp. 445–446.

[17] N. Balabanian and T. A. Bickart, *Linear Network Theory*. Beaverton, OR: Matrix, 1981, p. 465.

[18] HP-ADS, Hewlett Packard, EESOF Divison, "Advanced Design System 1.0," Tech. Rep., 1998.

[19] L. Zhao, A. C. Cangellaris, and J. L. Prince, *Reduced-Order Modeling of Electromagnetic Systems*: Univ. Arizona, Ctr. Electron. Packag. Res. (CEPR) software manual, Oct. 1998.

[20] D. M. Pozar, *Microwave Engineering*. Reading, MA: Addison-Wesley, 1990.

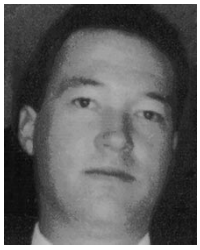

Mark Elzinga received the B.S.E.E. and the M.S.E.E. degrees from the University of Arizona, Tucson, in 1997 and 1999, respectively.

He has been a Research Assistant with the Center for Electronic Packaging Research since he started his graduate studies in the Electrical and Computer Engineering Department at the University of Arizona. As an undergraduate, he worked as a Student Engineer for Hughes Missile Systems Company in the Hybrid Microelectronics Division. In 1994, he and a partner formed a corporation, Animated Technology Inc., where he has been developing a proprietary high-speed three–dimensional animation system as well as consulting for other businesses. He now works at Intel Corporation. His interests include interconnect modeling, computational electromagnetics, CAD tool development, high-speed circuit design, packaging, digital design, microprocessors, computer graphics, and C++ programming.

Kathleen L. Virga (S'85–M'87–SM'97) received the B.S. degree from California State University, Long Beach, in 1985, the M.S. degree from California State University, Northridge, in 1987, and the Ph.D. degree from the University of California at Los Angeles (UCLA) in 1996, all in electrical engineering.

She is currently an Assistant Professor in the Electrical and Computer Engineering Department at the University of Arizona, Tucson. From 1985 to 1996, she worked in the Radar Systems Group, Hughes Electronics Electromagnetic Systems and Solid State Microwave Laboratories. Her work experience includes the design and development of phase shifters, RF feed networks, radiator elements, and transmit/receive (T/R) modules for airborne phased-array and active array antennas. Her current research interests include high-density circuit design packaging and interconnects as well as the development of novel antennas for radar and wireless communications systems. She holds 4 U.S. patents and has authored or coauthored over 25 technical publications.

Dr. Virga was awarded a Hughes Aircraft Company Doctoral Fellowship. She is a member of the IEEE Antennas and Propagation (AP-S) and Microwave Theory and Techniques (MTT) Societies, USNC-URSI Commission B, Eta Kappa Nu, Tau Beta Pi, and Sigma Xi. In 1999, she was elected to serve a three-year term on the Administrative Committee (AdCom) for the IEEE Antennas and Propagation Society. From 1997 to 1999, she was the PACE (Professional Activities) Chair for the AP-S Society and the Associate Editor responsible for the PACE column for the AP-S *Magazine*. In 1996, she received the UCLA Department of Electrical Engineering Graduate Woman of the Year award. She was the invited keynote speaker for the 1996 California State University Northridge, School of Engineering commencement.

John L. Prince (S'65–M'68–SM'78–F'90) received the B.S.E.E. degree from Southern Methodist University, Dallas, TX, and as an NSF Graduate Fellow received the M.S.E.E and Ph.D. degrees in electrical engineering from North Carolina State University, Raleigh.

He is currently Professor of Electrical and Computer Engineering and Director of the Center for Electronic Packaging Research at the University of Arizona, Tucson. He came to the University of Arizona in 1983. He has been Principal Investigator of the Semiconductor Research Corporation (SRC) Program in VLSI Packaging and Interconnection Research at the university since 1984. During 1991–1992, he was Acting Director, Packaging Sciences at SRC. He has extensive industrial experience. He is active in consulting work in both the reliability and packaging areas. He is coauthor on two books in the field of electronic packaging, *Simultaneous Switching Noise of CMOS Devices and Systems*, by Senthinathan and Prince, and *Electronic Packaging: Design, Materials, Processing and Reliability*, by Lau, Wong, Prince, and Nakayama. He teaches a course in electronic packaging at the University of Arizona. His current research interests center on developing modeling and simulation techniques for switching noise in packages and MCMs, on modeling and simulation techniques for mixed-signal system packaging, and on developing high-frequency measurements on packaging structures. He is the author or coauthor of over 150 papers in the field of electronic packaging, and 30 papers in the fields of semiconductor device physics, process development, and reliability.